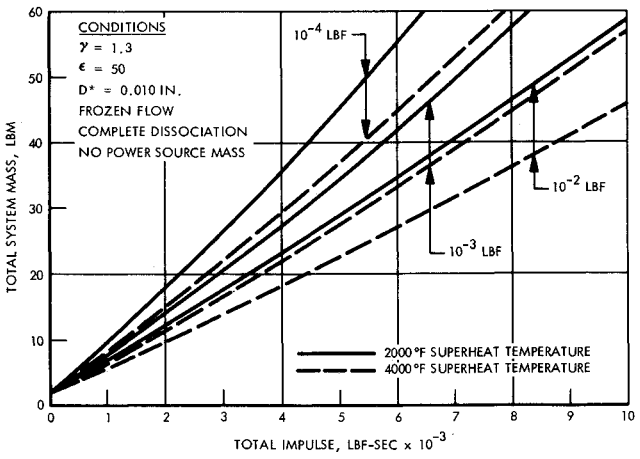


**Fig. 5 Total propulsion system mass vs total impulse for ammonium carbamate.**

shown in Fig. 3 (bottom) over a fairly wide range of operating conditions indicates that the performance of superheated ammonium carbamate should be predictable to within approximately ±5%.

A general relationship for throat Reynolds number is given in Ref. 1 as $Re^* = 4F/\pi\mu D^*\phi_{sp}I_{spt}$, where $D^*$ = throat diameter, $F$ = thrust, $I_{spt}$ = theoretical specific impulse, $\mu$ = viscosity, and $\phi_{sp} = I_{sp}/I_{spt}$. Using values of $\phi_{sp}$ from Ref. 1, Fig. 4 was obtained to show the relationship between thrust, throat diameter, nozzle pressure, and delivered specific impulse for temperatures of 2000 and 4000°F. The range of delivered specific impulse values for each $Re^*$ corresponds to the degree of dissociation obtained. The low number is for no dissociation while the high number is for complete dissociation. It is likely that complete dissociation would be obtained at 4000°F. Figure 4 illustrates the improvement in specific impulse obtained by decreasing the throat diameter for a particular value of thrust. It also shows that a portion of the improvement in the theoretical specific impulse obtained by an increase in temperature is offset by a reduction in $Re^*$, and hence $\phi_{sp}$, for the same $D^*$ and $F$. The reduction in $Re^*$ occurs through the decreased mass flow rate and increased viscosity associated with an increase in temperature.

From Fig. 4 it is apparent that specification of the propulsion system mass will be dependent on $F$, $D^*$, and temperature for $Re^* < 10^4$. Figure 5 illustrates this dependence for ammonium carbamate at the stated conditions. The choice of a 10-mil nozzle was somewhat arbitrary and the performance at the lowest thrust levels could be improved by using a smaller diameter if this were acceptable. The saving in mass with an increase of superheated gas temperature from 2000 to 4000°F is on the order of 30%. An assessment of the power source mass must also be made if this would not normally be available—as has been assumed in Fig. 5.

The total power requirement can be estimated from Fig. 1 by multiplying the theoretical total $P/F$ by $F/\phi_{sp}$. In addition to this, the propellant container and superheater losses must be supplied as well as power for flow control. If a valveless design were used, an additional 1 to 5 w would be required, depending on the operating conditions.[1,9]

### Conclusions

High-performance superheated sublimining solid thrusters are feasible by using present resistojet technology to materially increase the specific impulse. Performance comparable to that of $NH_3$ systems is possible when operated at the same conditions. Where thrust-response times on the order of minutes are acceptable, the 15 to 20% higher $I_{sp}$ for $NH_3$ resistojets can be offset by the increased reliability associated with a valveless subliming solid thruster.

### References

[1] Owens, W. L., Jr., "Design Aspects of Subliming Solid Reaction Control Systems," AIAA Paper 68-516, Atlantic City, N.J., June, 1968.

[2] White, A. F., "Electrothermal Microthrust Systems," AIAA Paper 67-423, Washington, D.C., 1967.

[3] Pugmire, T. K., Davis, W. S., and Lund, W., "ATS-III Resistojet Thruster System Performance," *Journal of Spacecraft and Rockets*, Vol. 6, No. 7, July 1969, pp. 790–794.

[4] Krieve, W. F., "Attitude Control and Stationkeeping Subsystem Program, Final Report," TR AFAPL-TR-68-14, March 1968, TRW Systems Group, Redondo Beach, Calif.

[5] Page, R. J. and Short, R. A., "Ten-Millipound Resistojet Performance," *Journal of Spacecraft and Rockets*, Vol. 5, No. 7, July 1968, pp. 857–858.

[6] Cutler, W. H., "Development of a Microthrust Stand for Direct Thrust Measurement," AIAA Paper 68-577, Cleveland, Ohio, June, 1968.

[7] Kanning, G., "Measured Performance of Water Vapor Jets for Space Vehicle Attitude Control Systems," TN-D-3561, Aug. 1966, NASA.

[8] Morin, R., private communication, Jan. 1970, Société Européene de Propulsion, Bordeaux, France.

[9] Owens, W. L., Jr., "A Flow Control Valve Without Moving Parts," *Proceedings of Fourth Aerospace Mechanisms Symposium*, May 22–23, 1969, Univ. of Santa Clara, Santa Clara, Calif.

# An Experimental and Analytical Study of Film Boiling Heat Transfer to Hydrogen

B. L. Pierce* and J. W. H. Chi†
*Westinghouse Electric Corporation, Pittsburgh, Pa.*

EARLY experimental studies on boiling heat transfer to hydrogen involved the measurement of heat fluxes and wall temperatures only. Core et al.[1] and Wright and Walters[2] studied both the nucleate and film boiling regimes but did not correlate their data. Hendricks et al.[3] studied the film boiling regime only and assumed an annular flow model and vapor-liquid equilibrium. They correlated a portion of their data through the use of the Martinelli parameter. In an early attempt to use this correlation to predict fluid and wall temperatures and fluid qualities, we found significant discrepancies between observed and predicted values. Similar results were found by Chenoweth et. al.[4]

Presented as Paper 70-660 at the AIAA 6th Propulsion Joint Specialist Conference, San Diego, Calif., June 15–19, 1970; submitted October 16, 1970; revision received February 28, 1971. The Nuclear Engine Rocket Vehicle Application Program (NERVA) is administered by the Space Nuclear Propulsion Office, a joint office of U.S. Atomic Energy Commission and NASA. Aerojet-General Corporation as prime contractor for the engine system and Westinghouse Electric Corporation as subcontractor for the nuclear subsystem, are developing a nuclear propulsion system for space applications. The authors wish to thank E. A. DeZubay who directed the experimental phases of this work, R. W. Graham and J. J. Watt of NASA, J. D. Rogers of LASL, and R. V. Smith of NBS Cryogenic Engineering Laboratory for many helpful discussions during various phases of this program.

* Fellow Engineer, Systems Engineering, Astronuclear Laboratory.

† Fellow Engineer, Power and Propulsion, Astronuclear Laboratory.

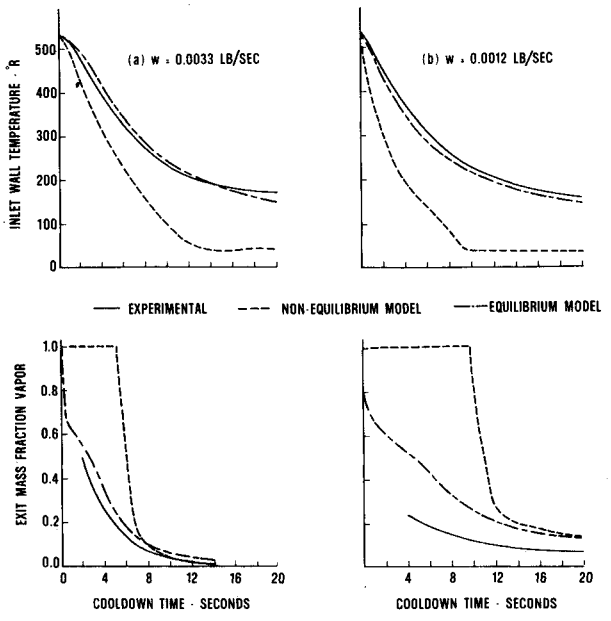


**Fig. 1 Comparison of wall temperature and exit vapor mass fraction histories.**

In studies on the cooldown of single tubes by hydrogen and nitrogen, Chi[5–8] showed that the film-boiling regime, which covers a major portion of a cooldown process, is dominated by mist and slug flows and significant departures from thermodynamic equilibrium were observed. This suggested that a simple annular flow model would be inadequate for film boiling heat-transfer calculations and a more general correlation was proposed.[8] The correlation, based on the superposition of a boiling term on a convective heat flux term, was shown to be applicable to single-phase vapor, mist flow, slug flow, and annular flow.

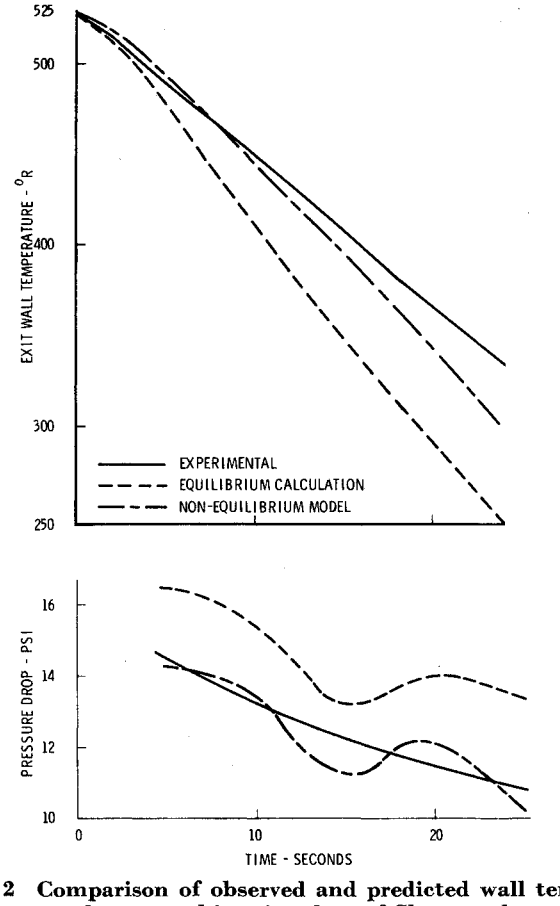


**Fig. 2 Comparison of observed and predicted wall temperature and pressure histories, data of Chenoweth et al.[4]**

As a part of those studies, transient wall and fluid temperatures, pressures, and flowrates were measured. This paper summarizes some of the results and describes a new analytical model for forced convective hydrogen film boiling heat-transfer calculations. The experimental data are compared with those predicted from the analysis.

## Experimental Equipment and Results

The cryogenic test loop was described in Ref. 8. The test sections consisted of $\frac{3}{16}$-in.-i.d. × 26-in.-long copper and aluminum tubes. Liquid hydrogen ($LH_2$) was stored in a "super-insulated" dewar, connected by vacuum-jacketed piping to the test section. Just preceding the test section were the gas purge lines, bypass valves, a 10-in.-long jacketed connector, and a glass section $5\frac{1}{2}$ in. long. The test section was mounted horizontally by spiders and rods in a vacuum chamber, two sides of which were plexiglas. Downstream piping, no vacuum-jacketed, contained the remotely controlled exit throttle valve, a standard gas orifice meter, and a vent. The piping upstream of the orifice meter was heated by heating tape to assure complete evaporation to gaseous $H_2(GH_2)$.

The test section and test loop were instrumented with an orifice meter, pressure transducers, and copper-constantan thermocouples to measure local wall and stream temperatures. The outputs were recorded continuously on a high-speed Minneapolis-Honeywell recording oscillograph (Visicorder®) at 4 in./sec. The Dewar pressure was varied (up to 60 psia) to yield different flow rates.

The experimental procedure consisted of 1) evacuation of the test loop and vacuum chamber, 2) purging the loop with $GN_2$ and $GH_2$, 3) precooling the loop up to the test section with $GH_2$ at $LN_2$ temperature by diverting the flow through the bypass, 4) cooldown of the loop up to the test section by $LH_2$, and 5) cooldown of the test section by pressurized $LH_2$. The test section was isolated from the rest of the test loop after the $GH_2$ purge to maintain it at ambient temperature. After complete cooldown of the loop piping, the coolant was introduced through the test section.

Oscillograph traces showed that the cooldown process is accompanied by temperature, pressure, and flow oscillations. The fluid temperature traces included high-amplitude, low-frequency oscillations, characterized by the intermittent appearance of a constant minimum temperature of finite duration, suggesting slug flow, and low-amplitude, high-frequency oscillations attributed to mist flow. A one-to-one correspondence among the temperature, pressure, and flow oscillations was evidenced by the peaks of the amplitudes. Simultaneous occurrences of mist and slug flows at different axial positions were observed in all cases. At any instant, the modes of two-phase flow along the axial length of the test section showed a sequence in reverse to that observed with time at any fixed position.

During a major portion of the cooldown process, the two-phase state departs appreciably from thermodynamic equilibrium conditions, i.e., superheated vapor exists simultaneously with the liquid. This may be expected from the relatively high specific heat of $GH_2$ and the relatively high wall-to-liquid temperature drops involved. Previous unsuccessful attempts to predict cooldown temperatures and two-phase fluid states may therefore be attributed to two poor assumptions: 1) annular flow and 2) thermodynamic equilibrium.

## Physical and Analytical Model

The temperature histories indicate that the heat flux increases steadily to a maximum, after which film boiling begins. With increasing chilldown, the heat flux decreases to a minimum and then increases suddenly to a second maximum

corresponding to the "critical" heat flux in boiling water systems and the commencement of nucleate boiling. These phenomena are analogous to those generally observed in pool-boiling.[5]

The equations of continuity, energy, and momentum may be written in the forms

$$-\partial G/\partial X = \partial \rho/\partial t \quad (1)$$

$$\pi D(q/A) - \rho A U \partial H/\partial X = -A\partial P/\partial t + \rho A \partial H/\partial t \quad (2)$$

and

$$\partial P/\partial X = (\rho/g)(\partial U/\partial t) - \rho(U/g)(\partial U/\partial X) - 2f\rho U^2/g\mathrm{D} \quad (3)$$

where $G$ is the instantaneous local mass velocity, $X$ is the axial distance, $\rho$ is the instantaneous local density, $t$ is time, $U$ is the mean longitudinal velocity, $P$ is the local pressure, $H$ is the total fluid enthalpy, and $A$ is the surface area. The equation of conduction for the test section is

$$\partial T/\partial t = \alpha[\partial^2 T/\partial r^2 + 1/r(\partial T/\partial r) + \partial^2 T/\partial X^2] \quad (4)$$

where $r$ is the radial position. When Eqs. (1-3) are converted to finite-difference forms, we have

$$G_{j,i+1} = G_{j-1,} - (\Delta X/\Delta t)(\rho_{j,i+1} - \rho_{j,i}) \quad (5)$$

$$H_{j,i+1} = \left[H_{j-i,i+1} + \frac{\Delta X}{\Delta t}\left(\frac{H_{j,i}}{U_{j,i}} + \frac{P_{j,i+1} - P_{j,i}}{G_{j,i}}\right) + \frac{D\pi\Delta X(q/A)}{w}\right]\frac{1}{1 + \Delta X/\Delta t U_{j,i}} \quad (6)$$

and

$$P_{j,i+1} = P_{j-1,i+1} + \Delta X/g\Delta t[G_{j,i} - G_{j,i+1} + G_{j,i}\rho_{i,j}(v_{j,i} - v_{j,i+1})] + G_{j,i}v_{j,i}(G_{j,i} - G_{j,i+1}) + G^2j,i(v_{j-1,i+2}v_{j,i+1}) = G_{j,i}{}^2 f\Delta x/\rho_{j,i}D_g \quad (7)$$

where the subscript $i$ denotes the time increment index and $j$ the space increment index.

The test section was divided into $n$ nodes. In place of Eq. (4), a heat balance equation was written for each node as follows:

$$q'''\Delta V + \frac{kA}{\Delta r}(T_{wj} - T_j) + \frac{kS}{\Delta X}(T_{j+i} - T_j) + \frac{kS}{\Delta X}(T_{j-1} - T_j) = \frac{\rho C\Delta V}{\Delta t}(T_j - T_j{}^*) \quad (8)$$

where subscript $w$ indicates the wall, $q'''$ is the heat generated per unit volume, $C_p$ is the heat capacity, $V$ is the volume, and $T^*$ denotes the previous node temperature.

### *Vaporization and superheat*

The inlet conditions are known for a space increment. For a slug of vapor in that increment, the temperature rise in the increment is found from

$$H_{v,j+1} = H_{v,j} + (q/A)_v D\Delta X/\dot{w} \quad (9)$$

where $\dot{w}$ is the flow rate, and

$$(q/A)_v = h_v(T_w - T_v) \quad (10)$$

Next, we calculate the average enthalpy $H_{j+1}$ over the time increment from Eq. (6). Then, we assume that any liquid that is vaporized must be superheated to the mean temperature of the vapor slug as calculated by Eq. (9). The vapor mass fraction is then

$$\chi_{j+1} = (H_{j+1} - H_L)/(H_{vj+1} - H_L) \quad (11)$$

The heat that goes into vaporizing the liquid in that space increment is

$$q = (\chi_{j+1} - \chi_i)\lambda\dot{w} \quad (12)$$

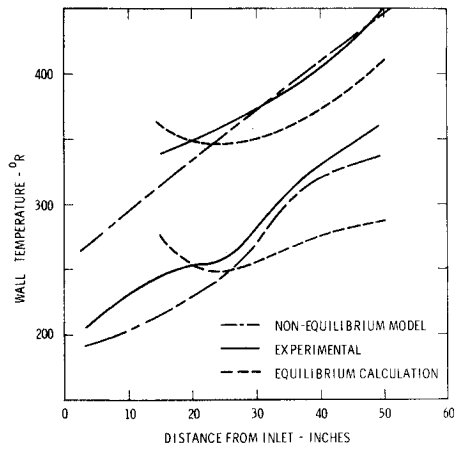


**Fig. 3 Comparison of observed and predicted axial wall temperature distributions during cooldown, NASA data.[4]**

where $\lambda$ is the latent heat of vaporization. These equations were programed in FORTRAN IV for the CDC 6600 computer.

### Comparison of Experimental Data with Analytical Results

Transient data were obtained from cooldown of metal test sections in this investigation and from Chenoweth et al.[4] in an independent study. Steady-state data were obtained by Hendricks et al.[3] in a study of boiling heat transfer to hydrogen. The "experimental" vapor fractions were estimated by the slug flow method.[5] Figure 1 compares the wall and fluid temperatures and the vapor qualities with those predicted by a) the assumption of thermodynamic equilibrium (all the heat transferred goes to vaporize the liquid) and b) the present nonequilibrium model. The former overpredicts cooldown and vapor qualities, whereas the latter gives curves in good agreement with the experimental values. The vapor qualities predicted by this model are somewhat higher than the estimated experimental values. However, the excellent agreement in observed and predicted wall and fluid temperatures suggest that more confidence can be placed in the predicted vapor qualities than those estimated from plug-slug flow theory. Nevertheless, the general trends of the quality histories are in excellent agreement and the new model represents a significant improvement over the equilibrium model.

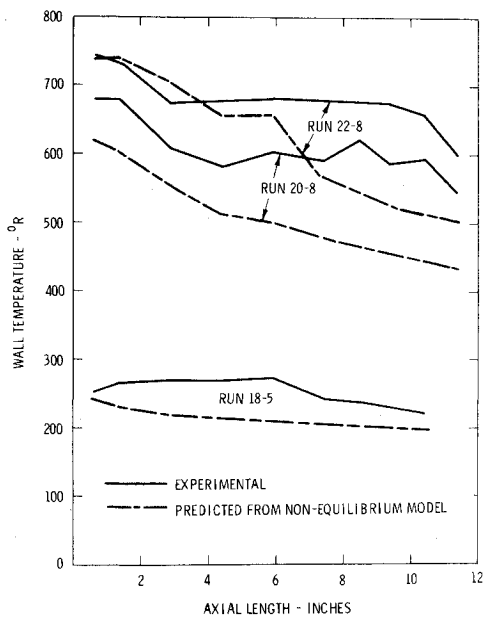


**Fig. 4 Comparison of observed and calculated steady-state axial temperatures, data of Hendricks et al.[3]**

Figure 2 compares typical temperature and pressure-drop histories from Ref. 4 with those predicted by the models. Again, the nonequilibrium model gives significantly improved predictions. Figure 3 compares axial $T_w$ distributions at two different cooldown times with similar results. Steady-state boiling heat-transfer data[3] provides another independent check on the analytical model. Predicted wall temperature distributions for three tests (Fig. 4) are low, but the general trends and the magnitudes are in good agreement. This suggests that the inlet conditions assumed are probably in error (following Hendricks, it was assumed that the inlet fluid was 100% liquid). Axial heat conduction upstream probably caused some prevaporization of liquid. The higher actual vapor qualities should lead to lower effective heat-transfer coefficients and thus higher wall temperatures.

### Discussions

It was recognized that the correct measurement of the bulk fluid temperature depends on the slug frequency (in mist and slug flows) and on the thermocouple and galvanometer response times. An analysis showed that the maximum thermocouple and galvanometer response times for the conditions studied is approximately 5 msec; hence slug flow with slug frequencies as high as 100 may be detected.

For the chilldown of the Cu test section, the maximum slug frequency observed was ~30. In general, the frequency was on the order of 2.5 or less. The liquid slug residence times increased with chilldown; the minimum occurring at the initiation of chilldown was on the order of 10–20 sec. Vapor slug residence times, on the other hand, remained at a high level throughout film boiling. Under these conditions, liquid slugs can be readily detected; and true separated-phase temperatures in the film-boiling regime can be measured with negligible errors. The transient test approach used in this study permitted the determination of local heat-transfer data over a wide range of conditions with a minimum number of tests.

For the development of a general equation to predict forced convection film boiling, it was postulated that slug flow occurs with discrete slugs of vapor and liquid. Although the experimental data included transitions from single phase to mist flow and then to slug flow, the generally good agreement between observed and predicted transient and steady-state properties suggest that the idealized slug flow model is satisfactory for the general determination of forced convective film boiling heat flux and for heat-transfer calculations.

### References

[1] Core, T. C., Harkee, J. F., Misra, A., and Sato, K., "Heat Transfer Studies," WADD-60-239, 1959, Wright Air Development Div., Wright-Patterson Air Force Base, Ohio.

[2] Wright, C. C. and Walters, H. H., "Single Tube Heat Transfer Tests—Gaseous and Liquid Hydrogen," WADC-TR-59-423, 1959, Wright Air Development Center, Wright-Patterson Air Force Base, Ohio.

[3] Hendricks, R. C., Graham, R. W., Hsu, Y. Y., and Friedman, R., "Experimental Heat Transfer and Pressure Drop of Liquid Hydrogen Flowing Through a Heated Tube," TN-D-765, 1961, NASA.

[4] Chenoweth, F., Watt, J. J., and Sprague, E. L., "Transient Chilldown of a Single Thick-Walled Tube by Liquid and Gaseous Hydrogen," TND-4238, 1967, NASA.

[5] Chi, J. W. H. and Vetere, A. M., "Two-Phase Flow During Transient Boiling of Hydrogen and Determination of Non-Equilibrium Vapor Fractions," *Advances in Cryogenic Engineering*, Vol. 9, Plenum Press, New York, 1964.

[6] Chi, J. W. H., "Effect of Mist Flow on Cool-Down Temperatures and Cool-Down Time," *Advances in Cryogenic Engineering*, Vol. 10, Plenum Press, New York, 1965.

[7] Chi, J. W. H., "A Correlation for Forced Convection Heat Transfer to Hydrogen," *Journal of Spacecraft and Rockets*, Vol. 3, No. 1, Jan. 1966, pp. 150–152.

[8] Chi, J. W. H., "Slug Flow and Film Boiling of Hydrogen," *Journal of Spacecraft and Rockets*, Vol. 4, No. 10, Oct. 1967, pp. 1329–1332.

# Time-Dependent Solutions of Nonequilibrium Dissociating Flow past a Blunt Body

C. P. Li*
*Lockheed Electronics Company Inc., Houston, Texas*

### Introduction

ANALYSIS of the chemical nonequilibrium flow past a blunt body at hypersonic speed has received much attention in recent years. A number of numerical techniques have been developed and applied to this problem with considerable success. It appears, however, that some of the techniques are inherently restricted to a two-dimensional flowfield calculation due to the algebraic complexities involved or the prohibitive computing time consumed when flow asymmetries are considered.[1,2] The coupling of chemical kinetic equations with the fluid-dynamic equations apparently tends to worsen the numerical difficulty already existing in these techniques. This Note describes an alternative technique that is simple and fast compared to others and can be applied to calculate nonequilibrium blunt body flows at high angles of attack.

The time-dependent technique used in this study is based largely on the work of Moretti and others[3] on a three-dimensional ideal gas blunt body flow problem. The bow shock is treated as a moving discontinuous surface and the computation of the flowfield is confined within a region bounded by the shock and body. A set of unsteady governing equations in nonconservative form is chosen and its asymptotic solution is considered to be the steady-state flowfield solution being sought. The continuous shock layer region is calculated by a second-order explicit finite-difference method, and boundary conditions at the shock and body are implemented using a quasi-one-dimensional, unsteady method of characteristics. The straightforward extension of Ref. 3 to account for the coupled dissociation-recombination processes is made by using three different equations: 1) an equation with pressure as the dependent variable, 2) an energy equation to replace the entropy equation, and 3) a chemical kinetic equation. For ease of computation and comparison with published data, an ideal dissociating diatomic gas model was selected for this paper. Numerical results discussed here include an oxygen gas flow past a sphere and a nitrogen gas flow past an ellipsoid at a 20° angle of attack. The results for oxygen flow past a sphere are compared with results obtained from a method of integral relations.[2]

Received December 9, 1970; revision received March 25, 1971. This work was supported by the Manned Spacecraft Center under NASA Contract 9-5384. The author gratefully acknowledges the help given by W. Reicks.

* Staff Engineer, Aeromechanics Section, Houston Aerospace Systems Division. Member AIAA.